Published in final edited form as:
Earth Syst Sci Data. 2018 ; 10(1): 87–107. doi:10.5194/essd-10-87-2018.

The Open-source Data Inventory for Anthropogenic Carbon dioxide (CO_2), version 2016 (ODIAC2016): A global, monthly fossil-fuel CO_2 gridded emission data product for tracer transport simulations and surface flux inversions

Tomohiro Oda[1,2], **Shamil Maksyutov**[3], **Robert J. Andres**[4]

[1]:Global Modeling and Assimilation Office, NASA Goddard Space Flight Center, Greenbelt, MD, USA

[2]:Goddard Earth Sciences Technology and Research, Universities Space Research Association, Columbia, MD, USA

[3]:Center for Global Environmental Research, National Institute for Environmental Studies, Tsukuba, Ibaraki, Japan

[4]:Carbon Dioxide Information Analysis Center, Oak Ridge National Laboratory, Oak Ridge, TN, USA

Abstract

The Open-source Data Inventory for Anthropogenic CO_2 (ODIAC) is a global high-spatial resolution gridded emission data product that distributes carbon dioxide (CO_2) emissions from fossil fuel combustion. The emission spatial distributions are estimated at a 1×1 km spatial resolution over land using power plant profiles (emission intensity and geographical location) and satellite-observed nighttime lights. This paper describes the year 2016 version of the ODIAC emission data product (ODIAC2016) and presents analyses that help guiding data users, especially for atmospheric CO_2 tracer transport simulations and flux inversion analysis. Since the original publication in 2011, we have made modifications to our emission modeling framework in order to deliver a comprehensive global gridded emission data product. Major changes from the 2011 publication are 1) the use of emissions estimates made by the Carbon Dioxide Information Analysis Center (CDIAC) at the Oak Ridge National Laboratory (ORNL) by fuel type (solid, liquid, gas, cement manufacturing, gas flaring and international aviation and marine bunkers), 2) the use of multiple spatial emission proxies by fuel type such as nightlight data specific to gas flaring and ship/aircraft fleet tracks and 3) the inclusion of emission temporal variations. Using global fuel consumption data, we extrapolated the CDIAC emissions estimates for the recent years and produced the ODIAC2016 emission data product that covers 2000–2015. Our emission data can be viewed as an extended version of CDIAC gridded emission data product, which should allow data users to impose global fossil fuel emissions in more comprehensive manner than original CDIAC product. Our new emission modeling framework allows us to produce future versions of ODIAC emission data product with a timely update. Such capability has become more significant given the CDIAC/ORNL's shutdown. ODIAC data product could play an important

Corresponding author: T. Oda (tomohiro.oda@nasa.gov).

role to support carbon cycle science, especially modeling studies with space-based CO_2 data collected near real time by ongoing carbon observing missions such as Japanese Greenhouse Observing SATellite (GOSAT), NASA's Orbiting Carbon Observatory 2 (OCO-2) and upcoming future missions. The ODIAC emission data product including the latest version of the ODIAC emission data (ODIAC2017, 2000–2016), is distributed from http://db.cger.nies.go.jp/dataset/ODIAC/ with a DOI.

1. Introduction

Carbon dioxide (CO_2) emissions from fossil fuel combustion are the main cause for the observed increase in atmospheric CO_2 concentration. The Carbon Dioxide Information Analysis Center (CDIAC) at the Oak Ridge National Laboratory (ORNL) estimated that the global total fossil fuel CO_2 emissions (FFCO2; fuel combustion, cement production and gas flaring) in the year 2014 was 9.855 PgC based on fuel statistics data published by United Nation (U.N.) (Boden et al., 2017). This FFCO2 estimate often serves as a reference in carbon budget analysis, especially for inferring CO_2 uptake by terrestrial biosphere and oceans (e.g. Ballantyne et al., 2012; Le Quéré et al., 2016). The Global Carbon Project for example estimated that approximately 55% of the carbon released to the atmosphere (FFCO2 plus emissions from land use change) was taken up by natural sinks over the past decade (2006–2015) (Le Quéré et al., 2016).

Similarly, FFCO2 estimates serve as a reference in atmospheric CO_2 flux inversion analysis where the location and size of natural sources and sinks are estimated using atmospheric CO_2 data and atmospheric transport models (e.g. Tans et al., 1990; Bousquet et al., 1999; Gurney et al., 2002; Baker et al., 2006). In the conventional inversion method, unlike land and oceanic fluxes, FFCO2 is a given quantity and never optimized (e.g. Gurney et al., 2005). FFCO2 thus needs to be accurately quantified and given in space and time to yield robust estimates of natural fluxes (Gurney et al., 2005). Accurately prescribing FFCO2 has become more critical because of the use of spatially and temporally dense CO_2 data from a wide variety of observational platforms (ground-based, aircrafts and satellites), which inform not only background levels of CO_2 concentration, but also CO_2 contributions from anthropogenic sources (e.g. Schneising et al., 2013; Janardanan et al., 2016; Hakkarainen et al., 2016). Atmospheric transport models then need to be run at a higher spatiotemporal resolution than before to fully interpret and utilized CO_2 variability observed at synoptic to local scale to quantify sources and sinks (e.g. Feng et al. 2016; Lauvaux et al., 2016). FFCO2 data thus needs to be accurately given at a high resolution so as not to cause biases in simulations.

Global FFCO2 data are available in a gridded form from different institutions and research groups (e.g. CDIAC/ORNL and Europe's Joint Research Center (JRC)) and those gridded emission data are often based on disaggregation of national (or sectoral) emissions (e.g. Andres et al., 1996; Rayner et al., 2010; Oda and Maksyutov 2011; Janssens-Maenhout et al., 2012; Kurokawa et al., 2013; Asefi-Najafabady et al., 2014). The emission spatial distributions are often estimated using spatial proxy data that approximate the location and intensity of human activities (hence, CO_2 emissions) (e.g. population, nighttime lights and

gross domestic production (GDP)) and/or geolocation of specific emission sources (e.g. power plant, transportation, cement production/industrial facilities and gas flares). CDIAC gridded emission data product for example is based on an emission disaggregation using population density at a 1×1 degree resolution (Andres et al., 1996). The Emission Database for Global Atmospheric Research (EDGAR, http://edgar.jrc.ec.europa.eu/) estimates emissions on the emission sectors specified by the Intergovernmental Panel on Climate Change (IPCC) methodology instead of fuel type and use spatial proxy data and geospatial data such as point and line source location at a 0.1×0.1 degree (Janssens-Maenhout et al., 2012).

Satellite-observed nighttime light data has been identified as an excellent spatial indicator for human settlements and intensities of some specific human activities (e.g. Elvidge et al., 1999, 2009) and has been used to infer the associated CO_2 emissions or their spatial distributions (e.g. Doll et al., 2000, Ghosh et al., 2010, Rayner et al., 2010). Oda and Maksyutov (2011) proposed a combined use of power plant profiles (power plant emission intensity and geographical location) and nighttime light data to achieve a global high-spatial resolution emission field. The decoupling of the point source emission which often have less spatial correlation with population (hence, nighttime light), yields improved high-resolution emission fields that show an improved agreement with the U.S. 10km Vulcan emission product developed by Gurney et al. (2009) (Oda and Maksyutov 2011). Based on Oda and Maksyutov (2011), we initiated the high-resolution emission data development (named as the Open-source Data Inventory for Anthropogenic CO_2, ODIAC) under the Japanese Greenhouse Gases Observing SATellite (GOSAT, Yokota et al., 2009) at the Japanese National Institute for Environmental Studies (NIES). The original purpose of the emission data development was to provide an accurate prior FFCO2 field for global and regional CO_2 inversions using the column-averaged CO_2 (XCO2) data collected by GOSAT. Since 2009, the ODIAC emission data product has been used for the inversion for the official GOSAT Level 4 (surface CO_2 flux) data production (Takagi et al., 2009; Maksyutov et al., 2013), NOAA's CarbonTracker (Peters et al., 2007) as a supplementary FFCO2 data, as well as dozens of published works (e.g. Saeki et al., 2013; Thompson et al., 2015; Feng et al., 2016; Feng et al., 2017; Shirai et al., 2017) including several urban scale modeling studies (e.g. Ganshin et al. 2010; Oda et al., 2012; Brioude et al., 2013; Lauvaux et al., 2016; Janardanan et al., 2016; Oda et al., 2017).

In response to increasing needs from the CO_2 modeling research community, we have upgraded and modified our modeling framework in order to produce a global, comprehensive emission data product on timely manner, while our flagship high-resolution emission modeling approach remains as the same. In this manuscript, we describe the year 2016 version of the ODIAC emission data product (ODIAC2016, 2000–2015), which was the latest version of the ODIAC emission data at the time of the submission of this manuscript, along with the emission modeling framework we are currently based on, highlighting changes/differences from Oda and Maksyutov (2011). Currently the updated, year 2017 version of the ODAIC emission data (ODIAC2017, 2000–2016) is available. This manuscript however provides the sufficient details of how we developed ODIAC2017 with updated information.

2. Emission modeling framework

Fig. 1 illustrates our current ODIAC emission modeling framework (we defined it as "ODIAC 3.0 model", in contrast to the original version). Major changes/differences from Oda and Maksyutov (2011, ODIAC v1.7) are 1) the use of emissions estimates made by the CDIAC/ORNL (rather than our own emission estimates), 2) the use of multiple spatial emission proxies in order to distribute CDIAC national emissions estimates made by fuel type, and 3) the inclusion of emission temporal variations (version 1.7 only indicates annual emission fields). Given CDIAC emission estimates have been one of well-respected, widely-used in the carbon research community (e.g. Ballantyne et al., 2012; Le Quéré et al., 2016), our philosophy in our emission data development is we develop and deliver an extended, comprehensive global gridded emission data product, fully utilizing CDIAC emissions data (e.g. emission estimates in both tabular and gridded forms). We also extend CDIAC emission data where possible. Our emission modeling framework was also designed to produce an annually-updated emission data product in a timely manner. Given the discontinuity of future, updated CDIAC emission data, we believe our emission data production capability of producing an extended product of the CDIAC emission data is significant.

Starting with national emission estimates as an input, our model framework achieves monthly, global FFCO2 gridded fields via preprocessing, and spatial and temporal disaggregation. CDIAC national estimates made by fuel type (liquid, gas, solid, cement production, gas flare and international bunker emissions) are further divided into an extended set of ODIAC emission categories (point source, non-point source, cement production, gas flare, international aviation and marine bunker (further described in Section 3). It is important to note that ODIAC2016 carries emissions from international bunker (international marine bunker and aviation, often accounts for a few percent of the global total emissions), which are not included in the CDIAC gridded emission data products (CDIAC gridded emission data only indicate national emissions and international bunker emissions are often not considered to be a part of national emissions in an international convention). With the inclusion of international bunker emissions, we provide a more comprehensive global gridded emission field. We extended the CDIAC national estimates over the recent years that was not yet covered in the version of CDIAC gridded data (2014–2016), in order to support near-real time CO_2 simulations/analysis. Emissions are then spatially distributed using a wide variety of spatial data (e.g. point source geographical location, nighttime light data and flight/ship tracks, further described in Section 4). We adopt an emission seasonality from existing emission inventories for particular emission categories (further described in Section 5).

In the following sections (Section 3–5), we describe how ODIAC2016 was developed. It is important to note that ODIAC2016 is based on the best available data at the time of the development (ODIAC2016 was released in September 2016). Thus, some of the emission estimates and underlying data used in ODIAC2016 might have been outdated. For traceability purpose, data used in this development, their versions/editions, and data sources are summarized in Appendix A. Following the results and evaluation section (Section 6), we discuss caveats and current limitations in our modeling framework/emission data product

(Section 7), and then describe how we will update the ODIAC emission data product with updated fuel statistics and/or emission information (Section 8). Atmospheric CO_2 inversion studies recently published (e.g. Maksyutov et al., 2013) and operational assimilation systems such as NOAA's Carbon Tracker (https://www.esrl.noaa.gov/gmd/ccgg/carbontracker/) often focus on time periods after 2000. We thus put a priority to produce emission data after year 2000 with regular update upon the availability of updated emission and fuel statistical data and deliver the emission product to the science community, instead of developing a longer term emission data product. Future versions of ODIAC data however might have a longer, extended time coverage. Currently the ODIAC data are provided in two data formats: 1) global 1×1 km (30 arc second) monthly data in the GeoTIFF format (only includes emissions over land) and 2) 1×1 degree annual (12 month) data in the NetCDF format (includes international bunker emissions). The 1×1 degree annual data are aggregated from the 1×1 km product. The improvements with the use of improved nighttime light data in the 1×1 km data were documented in Oda et al. (2012). This manuscript thus focuses on the comprehensive global FFCO2 fields at a 1×1 degree, otherwise specified.

3. Emission estimates and input emission data preprocessing

3.1 Emissions for 2000–2013

CDIAC FFCO2 emissions estimates are based on fuel statistic data published as United Nation Energy Statistics Database (Boden et al., 2017). Emission estimates are calculated on global, national and regional basis and by fuel type in the method described in Marland and Rotty (1984). CDIAC also provides their own gridded emission data products that indicate annual and monthly FFCO2 fields at a 1×1 degree (Andres et al., 1996; Andres et al., 2011). ODIAC2016 is primarily based on the year 2016 version of the CDIAC national estimates (Boden et al., 2016), which was the most up-to-date CDIAC emission estimates at the time of the data development (currently Boden et al. 2017 is the latest). We first aggregated the CDIAC national (and regional) emissions estimates to 65 countries and 6 geographical regions (North America, South and Central Americas, Europe and Eurasia, the Middle East, Africa, and Asia Pacific) defined in Oda and Maksyutov (2011) (see the country/region definitions are shown in Table 1 in Oda and Maksyutov 2011). In addition to the national and geographical categories, we decided to include Antarctic fishery emissions, which are from fishery activities over the Antarctic Ocean (< 60S, 1~ 4 kTC/yr over 1987–2007 by Boden et al., 2016), as an individual emission region and distributed in the same way as Andres et al. (1996). Emissions from international bunker and aviation are not included in national emissions by international convention. Thus CDIAC gridded emission data products do not include the emissions from international bunker and aviation although the CDIAC/ORNL does have records of those emissions on national/regional basis. ODIAC2016 includes those emissions to achieve comprehensive global FFCO2 gridded emission fields.

In CDIAC emission estimates, the global total emission and national total emissions are obtained by different calculation methods (global fuel production vs. apparent national fuel consumption, see Andres et al., 2012) and the CDIAC national totals do not sum to the CDIAC global total due to the difference in calculation method and inconsistencies in the underlying statistical data (e.g. import/export totals) (e.g. Andres et al., 2012). We thus

calculate the difference between the global total and the sum of national totals and scaled up national totals to account for the difference. Andres et al. (2014) reported global total emission estimates calculated with production data (as opposed to apparent consumption data) have the smallest uncertainty (approximately 8% (2 sigma). It is thus used as the reference for global carbon budget analyses (e.g. Le Quéré et al., 2016). Inversion analysis is an extended version of the global carbon budget analysis using atmospheric models. We thus believe that imposing transport models and/or inversion models in a consistent way with the global carbon budget analysis such as Le Quéré et al. (2016) has significance, although we sacrifice the accuracy of the national/regional emission estimates. Due to the global scaling, national totals in ODIAC2016 differ from the estimates originally reported by the CDIAC/ORNL. The differences between the CDIAC global total and the sum of national emissions are often few percent and thus the magnitude of the scaling is often within the uncertainty range of national emissions (e.g. 4.0 to 20.2%, Andres et al., 2014). The global scaling factor derived and used in this study are presented in Appendix A2.

3.2 Emissions for 2014–2015

The year 2016 version of the CDIAC emission estimates only covers years to 2013 (Boden et al., 2016). We thus extrapolated the year 2013 CDIAC emissions to years 2014 and 2015 using the year 2016 version of the BP global fuel statistical data (BP, 2017). Our emission extrapolation approach is the same as Myhre et al. (2009) and Le Quéré et al. (2016). Emissions from cement production and gas flaring (approximately 5.7% and 0.6% of the 2013 global total, Boden et al., 2016) were assumed to be as the same as year 2013. International bunker emissions were scaled using changes in national total emissions.

3.3 CDIAC emission sector to ODIAC emission categories

CDIAC national emission estimates (prepared by fuel type) were re-categorized to our own ODIAC emission categories (point source, nonpoint source, cement production, gas flare and international aviation and international marine bunker). Following Oda and Maksyutov (2011), the sum of emissions from liquid, gas and solid fuels was further divided into point source emissions and non-point source emissions. The total emissions from point sources were estimated using national total power plant emissions calculated using CARMA (Oda and Maksyutov, 2011). As mentioned earlier, CDIAC gridded emission data products only indicate national emissions and do not include international bunker emissions (Andres et al., 1996, Andres et al., 2011). In contrast, EDGAR provides bunker emissions in their gridded data product (JRC, 2017). Peylin et al. (2013) show some models include international bunker emissions and some do not, although the difference due to the inclusion/exclusion of the international bunker emissions in the prescribed emissions could be corrected afterwards (Peylin et al., 2013). In ODIAC2016, we carry CDIAC international bunker emissions reported on country basis to achieve the complete picture of the global fossil fuel emissions. Country total bunker emissions (aviation plus marine bunker) were distributed using spatial proxy data adopted from other emission inventories described later (see Section 4.3). Although the CDIAC/ORNL does not report emissions from international aviation and marine bunker separately, we loosely estimated those two emissions using U.N. statistics. We estimated the fraction of aircraft emissions using jet fuel and aviation gasoline

consumption and then the international bunker emissions were divided into aircraft and marine bunker emissions.

4. Spatial emission disaggregation

4.1 Emissions from point sources, non-point sources and cement production

We define the sum of the emissions from solid, liquid and gas fuels as land emission (see Fig. 1). Land emissions are further divided into two emission categories (point source emissions and non-point source emissions) and then distributed at a 1×1 km resolution in the ways described in Oda and Maksyutov (2011): Point source emissions are mapped using power plant profiles (emission intensity and geographical location) taken from the CARbon Monitoring and Action (CARMA) database (Wheeler and Ummel, 2008) and non-point source emissions are distributed using nighttime light data collected by the Defense Meteorological Satellite Program (DMSP) satellites (e.g. Elvidge et al., 1999). To avoid a difficulty in emission disaggregation especially over bright regions in nighttime light data (e.g. cities), Oda and Maksyutov (2011) employed a product that does not have an instrument saturation issue, rather than regular nightlight product. ODIAC2016 employs the latest version of the special nighttime light product (Ziskin et al., 2010). The improved nighttime light data has mitigated the underestimation of emissions over dimmer areas seen in ODIAC v1.7 (Oda et al., 2010). Nighttime light data are currently available for multiple years (1996–97, 1999, 2000, 2002–03, 2004, 2005–06 and 2010). In ODIAC2016, due to the lack of information, the emissions from cement production were spatially distributed as a part of non-point source emissions, although those emissions should have been distributed as point sources. This needs to be fixed in future versions of ODIAC emission data.

4.2 Emissions from gas flaring

In the ODIAC v1.7, emissions from gas flaring were not considered (Oda and Maksyutov 2011). Nighttime light pixels corresponding to gas flares often appear very bright and would result in creating strong point sources in emission data (Oda and Maksyutov, 2011). We thus identified and excluded those bright gas flare pixels before distributing land emissions, using another global nighttime light data product that was specifically developed for gas flares by National Oceanic and Atmosphere Administration (NOAA), National Centers for Environmental Information (NCEI, former National Geophysical Data Center (NGDC)) (Oda and Maksyutov, 2011). In ODIAC2016 we separately distributed CDIAC gas flare emissions using the 1×1 km nightlight-based gas flare maps developed for 65 individual countries (Elvidge et al., 2009). Other than the 65 countries, the gas flare emissions were distributed as a part of land emissions.

4.3 Emissions from international aviation and marine bunker

Emissions from international aviation and marine bunker were distributed using aircraft and ship fleet tracks. International aviation emissions were distributed using the AERO2k inventory (Eyers et al., 2005). The AERO2k inventory was developed by a team at the Manchester Metropolitan University (MMU) and indicates the fuel use and NOx, CO_2, CO, hydrocarbon and particulate emissions for 2002 and 2025 (projected) with injection height at a 1×1 degree spatial resolution on monthly basis. We used their column total CO_2 emissions

to distribute emissions to a single layer. International marine bunker emissions were distributed at a 0.1×0.1 degree using an international marine bunker emission map from the EDGAR v4.1(JRC, 2017). We decided not to adopt an international and domestic shipping (1A3d) map from EDGAR v4.2 as it includes domestic shipping emissions that we does not distinguish.

5. Temporal emission disaggregation

The inclusion of the temporal variations is often a key in transport model simulation. For CO_2 flux inversion, the potential biases in flux inverse emission estimates due to the lack of temporal profiles was suggested by Gurney et al. (2005). In ODIAC2016, we adopt the seasonal emission changes developed by Andres et al. (2011). The CDIAC monthly gridded data include monthly national emissions gridded at a 1×1 degree resolution (Andres et al. 2011). We normalized the monthly emission fields by the annual total and the applied to our annual emissions over land. The seasonality in ODIAC2016 is based on the year 2013 version of the CDIAC monthly gridded emission. The CDIAC monthly emission data do not cover the recent years. For recent years, we created a climatological seasonality using monthly CDIAC data from 2000–2010 (excepting 2009 where economic recession happened). Due to the limited availability of monthly fuel statistical data, Andres et al. (2011) used proxy country and also seasonality allocated by Monte Carlo simulations. The years between 2000–2010 were most data rich period and mostly explained by data (see Fig. 1 in Andres et al., 2011).

Although ODIAC2016 only provides monthly emission fields, users can derive hourly emissions by applying scaling factors developed by Nassar et al. (2013). The Temporal Improvements for Modeling Emissions by Scaling (TIMES) is a set of scaling factors which one can derive weekly emissions and diurnal emissions from any monthly emission data that you use. Temporal profiles are collected from Vulcan, EDGAR and best available information and gridded on a 0.25×0.25 degree (Nassar et al., 2013). TIMES also includes per capita emissions corrections for Canada (Nassar et al., 2013).

6. Results and discussions

6.1 Annual global emissions

In Fig. 2, global emission time series from different emission data were compared to give an idea of agreement among them. We calculated the global total for each year from four gridded emission data for the period of 2000–2016: CDIAC global total + projection (taken from ODIAC2016), CDIAC gridded data (hence, no international bunker emissions), two versions of EDGAR gridded data (v4.2 and FastTrack). The uncertainty range (shaded in tan) is 8% (2 sigma) estimated for CDIAC global by Andres et al. (2014). Those gridded emission data are often used in global atmospheric CO_2 inversion analysis (e.g. Peylin et al., 2013). To account for the difference in emission reporting categories (e.g. fuel basis in CDIAC vs. emission sector basis in EDGAR), the EDGAR totals were calculated as the “total short cycle C” emissions minus the sum of emissions from agriculture (IPCC code: 4C and 4D), land use change and forestry (5A, C, D, F and 4E) and waste (6C) (see more details on emission sectors documented in JRC (2017)). International aviation (1A3a) and

navigation (1A3b) were thus included in values for EDGAR time series. The authors acknowledge the JRC has updated EDGAR emission time series for 1970–2012 in November 2014 (JRC, 2017). This study however uses gridded emission data, which are not fully based on the updated emission estimates, in order to characterize differences from gridded emission data, especially for potential data users in the modeling community.

All four global total values obtained from four gridded emission data agree well within 8% uncertainty. The difference between ODIAC and CDIAC gridded data (3.3%−5.7%) were largely attributable to the international bunker emissions and global correction. ODIAC (where the total was scaled by CDIAC global total) and two versions EDGAR showed minor differences in magnitude (0.3%−2.7%) and trend, which are largely attributable to the differences in the underlying statistical data (e.g. U.N. Stat vs. EIA from different inventory years) and the emission calculation method (fuel basis vs. sector basis). Global total estimates at 5-year increments are shown in Table 1. For the year 2014 and 2015, we estimated the global total emissions 9.836 and 9.844 PgC. Boden et al. (2017) reported the latest estimate for year 2014 global total emission as 9.855 PgC. Our projected 2014 emission estimate was lower than the latest estimate by approximately 0.02 PgC (0.2%).

Fig. 3 shows the same type of comparison as Fig. 2, but for the top 10 emitting countries (China, US, India, Russian Federation, Japan, Germany, Islamic Republic of Iran, Republic of Korea (South Korea), Saudi Arabia and Brazil, according to the year 2013 ranking reported by CDIAC). We aggregated all the four gridded emission fields to a common 1×1 degree field and sampled using the 1×1 degree country mask used in CDIAC emission data development. The annual uncertainty estimates for national total emissions (2 sigma) are made following the method described by Andres et al., (2014) and values are shown in Table 2. In the analysis presented in Fig. 3, emissions from international aviation (1A3a) and navigation (1A3b) are excluded. All four national total values sampled from four gridded emission data at a 1×1 degree often agree within the uncertainty estimated by Andres et al. (2014). Systematic differences of ODIAC from CDIAC gridded data can be largely explained by 1) global correction (the total was scaled using CDIAC global total) and 2) the differences in emissions disaggregation methods. Although ODIAC is expected to indicate slightly higher values than CDIAC gridded data (often a few percent) because of the global correction (note global correction can be negative, despite of the depiction in Fig. 1), ODIAC sometimes indicates values lower that CDIAC gridded data more than few percent (see Japan in Fig. 3 as an example). This is due to a sampling error using the 1×1 degree country map in the analysis. The aggregated 1×1 degree ODIAC field is slightly larger than that of CDIAC especially because of the coastal areas depicted a high-resolution in the original 1×1 km emission field. This type of sampling error was discussed in Zhang et al. (2014). ODIAC employs a 1×1 km coastline and a 5×5 km country mask as described in Oda and Maksyutov (2011). Thus, the use of 1×1 degree CDIAC country map results in missing some land mass (hence, CO_2 emissions). Similar sampling errors can happen for countries that are physical small and island countries, depending on the resolution of analysis. Despite of the sampling errors, the authors used the CDIAC 1×1 degree country map to do this comparison analysis with having CDIAC gridded data as a reference. The lower emission indicated by ODIAC or EDGAR in this analysis does not always mean the

national total emissions are lower. The emission estimates at national level often agree well even among different emission inventories (e.g. Andres et al., 2012).

6.2 Global emission spatial distributions

The global total emission fields of CDIAC gridded emission data and ODIAC2016 for the year 2013 (the most recent year CDIAC indicates) are shown in Fig. 4. Emission fields are shown at a common 1×1 degree. The major difference seen between two fields is primarily due to inclusion/exclusion of emissions from international bunker emissions that largely account for the differences indicated in Table 1. A breakdown of ODIAC year 2013 emission field are presented by emission category in Fig. 5. The emission fields for point sources, non-point sources, cement production and gas flaring were produced at a 1×1 km resolution in ODIAC 3.0 model, but as mentioned earlier, we focus on the 1×1 degree version of ODIAC2016 in this manuscript. In CDIAC gridded emission data, the emissions over land are distributed by population data without fuel type distinction. In ODIAC 3.0 model, we have added additional layers of consideration in the emission modeling from the conventional CDIAC model and add the possibility of future improvement with improved emission proxy data.

In Fig. 6, we compared the four global gridded products over land and also calculated differences from ODIAC2016 (shown in Fig. 7. Histograms are presented in Appendix A3). It is often very challenging to evaluate the accuracy and uncertainty of gridded emission data, because of the lack of direct physical measurements at grid scales (Andres et al., 2016). Recent studies have attempted to evaluate the uncertainty of gridded emission data by comparing emission data each other (e.g. Oda et al., 2015; Hutchins et al., 2016). The differences among emission were used as a proxy for uncertainty. However, it is important note that such evaluation does not give us an objective measure of which one is closer to truth, beyond characterizing the differences in emission spatial patterns and magnitudes from methodological viewpoints (e.g. emission estimation and disaggregation). Some of the gridded emission data are partially disaggregated using commercial information, which users are often not authorized to fully disclose the information used and thus makes the comparison even less meaningful and/or significant. Oda et al. (2015) also discussed that emission inter-comparison approaches often do not allow us to evaluate two distinct uncertainty sources (emissions and disaggregation) separately. In addition, because of the use of emission proxy for emission disaggregation (rather than mechanistic modeling), such comparison can be only implemented at an aggregated, coarse spatial resolution. These issues will be further discussed in the Section 7.

Because of the limitation mentioned above, we here compared emission data only to characterize the differences that can be explained by the differences in emission disaggregation methods. We implemented this comparison exercise using 2008 emission field aggregated at a 1×1 degree resolution. Year 2008 is the most recent year where all the four emission fields are available. The major emission spatial patterns (e.g. emitting regions such as North America, Europe and East Asia) are overall very similar as the correlations were driven by national emission estimates (which we already saw good agreement earlier), but we do see differences due to emission disaggregation at the subnational level. Because of

the use of nightlight, ODIAC did not indicate emissions over some of the areas (e.g. Africa and Eurasia) while others do. Especially, EDGAR has emissions over those areas that are largely explained by line source emissions such as transportation. Overall, ODIAC tends to put more emissions towards populated areas than suburbs. This is also explained by the lack of line sources. In EDGAR v4.2, domestic fishery emissions can be seen, but not in EDGAR FT. Even in these two EDGAR versions, we can confirm the subnational differences at United States, Europe and China.

6.3 Regional emission time series.

Fig. 8 shows time series of regional fossil fuel emissions aggregated over 11 land regions defined in the TransCom transport model intercomparison experiment (e.g. Gurney et al., 2002). The global seasonal variation and the associated uncertainty have been presented and discussed in Andres et al. (2011). Here monthly total emission values were calculated for eleven TransCom land regions and presented with the associated uncertainty values (see Table 3). The monthly total values were calculated in both excluding international bunker emissions (hence, land emissions only) and including the emissions. The uncertainty range was calculated by mass weighted uncertainty estimates of countries that fall into the TransCom regions. The uncertainty ranges shown in Fig. 8 are annual uncertainty plus the monthly profile uncertainty (12.8%, reported by Andres et al., 2011). Monthly time series are presented for land only emissions and land and international bunker emission (here, largely aviation emissions). As described earlier, the emission seasonality was adopted from Andres et al. (2011). The patterns in the emission seasonality are often largely characterized by the large emitting countries within the regions (e.g. U.S. for region 2; China for region 8). Since Andres et al. (2011) used geographical closeness (also, type of economic systems) to define proxy countries, the countries in the same TransCom regions can have similar or the same seasonal patterns in their emissions.

As we can see in Fig. 4 (panel plot for aviation emissions), aviation emissions are intense over North America, Europe and Asia. Global total aviation emission was approximately 0.12 PgC/yr in 2013 and it often does not account for a large portion of the global total (1.2% of the global total in 2013). However, considering the fact that those emissions are concentrated in particular areas such as North America, Europe and East Asia, rather than evenly distributed in space, and often imposed at the surface layer in transport model simulation, care must be taken to achieve an accurate atmospheric CO_2 transport model simulation (Nassar et al., 2010). Aviation emissions were often around 0.5–5.1% of the land total emissions over the most regions, but as large as 12.7% (North American Boreal).

7. Current limitations, caveats and future prospects

As ODIAC emission data product is now used for a wide variety of the carbon cycle research (e.g. global, regional inversions, urban emission studies), it would be useful for the users of the ODIAC emission data product to note and discuss issues, limitations and caveats in our emission data that the authors are aware. Some of the issues and limitations are specific to our study, however the majority of them are often shared by other existing gridded emission data and or emission models.

7.1 Emission estimates

In the production of ODIAC2016, we used several versions/editions of CDIAC estimates (e.g. global estimates, national estimates and monthly gridded data). This could often happen in emission data production, as some of the underlying data are not updated/upgraded at the time of emission data production (we often start updating emission data after new fuel statistical data are released). We sometimes accept the inconsistency and try to use the most up-to-date information available. For example, we could use GCP's emission estimates (e.g. Le Quéré et al., 2016) to constrain the global totals, if CDIAC global total emission estimates are not available. The way we obtained emission estimates for each version is often described in the NetCDF header information of the emission data product. The use of the CARMA power plant estimates for estimating magnitude of point source portion of emissions is hard to eliminate, although ideally this is done using emission estimates that are fully compatible to CDIAC estimates. We are currently examining U.N. statistical data (which CDIAC emission estimates are based on) to assess the ability of explaining power plant emissions.

7.2 Emission spatial distributions

7.2.1 Point source emissions—Although the use of the power plant geolocation allowed us to achieve improved high-resolution emission spatial distributions over land (Oda and Maksyutov, 2011), the availability of power plant data is often very limited. For example, CARMA does not provide power plant emissions and its status (e.g. commission/decommission) every year and furthermore update/upgrade after their version 3.0 database (which dated 2012). The error in their power plant geolocation is another issue that has been identified (e.g. Oda and Maksytuov, 2011; Woodard et al., 2015). In ODIAC, the base year emissions (2007) were projected and all the power plants were assumed to be active over the period (Oda and Maksyutov, 2011). There are only few global projects that are collecting power plant information such as the Global Energy Observatory (GEO, http://globalenergyobservatory.org/) and those can be a useful source of data to improve and supplement CARMA database. Regionally, CARMA can be evaluated using an inventory such as the U.S. Emissions and Generation Resource Integrated Database (eGRID) (EPA, 2017). However, it is often difficult to find such a well-constructed and documented inventory for countries that are actually driving the uncertainty in global emissions (e.g. China and India).

Emissions from cement production (which are currently distributed using nightlight by Ziskin et al., 2010) and gas flare (which is distributed using gas flare nightlight data by Elvidge et al., 2009) should be distributed as point sources. For gas flare emissions, we are examining the use of Nightfire (Elvidge at al., 2013a) to pinpoint active gas flares in timely manner and improve their emissions spatial disaggregation over the recent years. Currently, the point source emissions in ODIAC do not have an injection height due to the lack of global information. This limitation is shared with other existing global emission data products.

7.2.2 Non-point source emissions—Nighttime light data has been an excellent proxy for human settlements (hence, CO_2 emissions) even at a high spatial resolution, however

there are some issues to be discussed. As mentioned earlier, we used an improved version of calibrated radiance data developed by Ziskin et al. (2010), but those data are only available to seven data periods over the course of DMSP years (1992–2013). As we do not believe linearly interpolating the existing nightlight data over the intervening years is necessarily the best way (as done in Asefi-Najafabady et al., 2014), the same nightlight data has been used for some periods and thus emission distributions remain unchanged. We are now examining the use of nightlight data collected from the Visible Infrared Imaging Radiometer Suite (VIIRS) on Suomi National Polar-orbiting Partnership satellite (e.g. Elvidge et al., 2013b; Roman and Stokes, 2015). VIIRS instruments do not have several critical issues that the DMSP instrument had (e.g. spatial resolution, dynamic range, quantization and calibration) (Elvidge et al., 2013b). The fully calibrated nightlight data can be used to map emission changes in space in timely and consistent manner.

In ODIAC, the disaggregation of non-point emissions is solely done using nighttime light data for estimating subnational emission spatial distributions and no additional subnational emission constrain were applied. Rayner et al. (2010) proposed to better constrain subnational emission spatial distribution by combining population data, nighttime lights and GDP in their Fossil Fuel Data Assimilation System (FFDAS) framework. Asefi-Najafabady et al. (2014) further introduced the use of point source information in their disaggregation, the optimization in their current framework is however under-constrained by the lack of GDP information. Without having such optimization, the state level per capita emission estimates can provide subnational constraints. Nassar et al. (2013) evaluated the per capita emissions in CDIAC and ODIAC emission data over Canada using the national inventory and found that ODIAC outperformed. However, as the nightlight-population relationship might have a bias for developing and the least developed countries (Raupach et al., 2010), we would expect we see significant biases over those countries and the per capita estimates can provide a useful constraint.

As seen in the comparison to other emission data, the major difference from EDGAR emission spatial distribution was due to the lack of line sources in ODIAC. We do not believe the result from the emission data comparison can falsify the emission distribution in ODIAC, as discussed earlier. However, we do expect an inclusion of the line sources would improve the spatial distributions and emission representations in both cities and rural areas. We are currently examining the inclusion of transportation network data (e.g. OpenStreetMap) as proxy for line source emissions to explore the better spatial emission aggregation method. Oda et al. (2017) recently implemented the idea of adding a spatial proxy for line sources and improved emission estimates for a U.S. city.

7.2.3. Aviation emissions—We estimated emissions from international aviation from CDIAC using U.N. statistical data. The emissions are currently provided as a single layer emission field, although it is not appropriate given the nature of the aviation emissions. Nassar et al. (2010) discussed that the importance of the three dimensional (e.g. x,y,z) emissions for interpreting CO_2 profile. In current modeling framework, although we maintain the aviation emission injection height from AERO2k (reduced to 1km interval), we distribute the emissions to a single layer. As pointed out by Olsen et al. (2013), AERO2k does not agree with other inventories in height distribution. With noting the caution, we will

examine the use of height information from AERO2k and other data available to us and do sensitivity analysis using transport model simulations.

7.3 Emission temporal profiles.

The emission seasonality in ODIAC2016 is based on Andres et al. (2011) and it can be further extended using the TIMES scaling parameter to hourly scale. We note that the emission seasonality was based on top 10 emitting countries' fuel statistics and Monte Carlo simulation (Andres et al., 2011). The emission seasonality for countries other than the top 10 could be less robust. Also, because of the use of Monte Carlo, the seasonality is different over different editions of monthly emission data. It is also important to note that the repeated use of climatological (mean) seasonality for the recent years (described in Section 5) could be a source of uncertainty and biases. Andres et al. (2011) estimated the monthly uncertainty as 12.8% (two sigma) in addition to the annual emission uncertainty. As we often impose fossil fuel emissions, a care must be taken when applied to inversions. Ultimately, as done by Vogel et al. (2013), we might be able to evaluate temporal profiles from statistical data and improve them (but only to limited small locations).

7.4 Uncertainties associated with gridded emission fields

As mentioned earlier, the evaluation of gridded emission data is often very challenging and most of the emission data study share this difficulty. Although the emission estimates are made at global and national scales with small uncertainties (e.g. 8% for global by Andres et al., 2014), considerable errors seem to be introduced when the emissions are disaggregated (e.g. Hogue et al., 2016; Andres et al., 2016). Andres et al. (2016) for example estimated the uncertainty associated with CDIAC gridded emission data on a per grid cell basis with an average of 120% and a range of 4.0 to 190% (2 sigma). Hogue et al. (2016) closely looked at CDIAC gridded emission data over the U. S. domain and estimated the uncertainty associated with the 1×1 degree emission grids as ±150%. Those errors seem to be unique to the disaggregation method (Andres et al., 2016). Future funding may allow us to pursue a full uncertainty analysis of the ODIAC emission data/model, akin to the Andres et al. (2016) approach but accounting for the greater than one carbon distribution mechanisms utilized in the ODIAC emission modeling framework. All of the spatially distributed gridded emission data mentioned in this manuscript suffer from the same basic defect: they use proxies to spatially distribute emissions rather than actual measurements. In addition, evaluating emission distributions based on a nightlight proxy can be challenging as the connection between CO_2 emissions and proxy is less direct compared to population (e.g. per capita emissions). A combined use of emission proxy and geolocation data (e.g. power plant location) would also add additional difficulties to give a comprehensive measure of the uncertainty because of different type of error/uncertainty sources (e.g. Woodard et al., 2015). As finer spatial scales are approached, the defect of the proxy approach becomes more apparent: proxies only estimate emission fields. The ODIAC data product has been used not only for global simulations at an aggregated spatial resolution, but also at very high spatial resolution (e.g. Ganshin et al. 2010; Oda et al. 2012; Lauvaux et al. 2016; Oda et al. 2017). Thus, an emission evaluation at a high resolution has become an important task. One approach we could take for evaluating high-resolution emission fields is comparing to a local fine-grained emission data product such as Gurney et al. (2012), acknowledging the

limitations of the approach discussed earlier. Another approach would be evaluating emission data in concentration space, rather than emission space. As reported in Vogel et al. (2013) and Lauvaux et al. (2016), with radiocarbon measurements and/or good, spatially dense CO_2 measurements, a high-resolution transport model simulation can provide an objective measure for emission data evaluations (e.g. model-observation mismatch and emission inverse estimate).

While the quality (i.e. bias and uncertainty) of the gridded emission estimates remains unquantified for most of the emission data mentioned in this manuscript, the emission data are still used because sufficient measurements in space and time are not presently available to offer a better alternative. At very least, we presented the uncertainty estimates over the aggregated TransCom land regions. We believe that the regional uncertainty estimates are highly useful for atmospheric CO_2 inversion modelers, more than uncertainty estimates at a grid level, which still do not seem to be ready for use. Inversion studies often aggregate flux estimates over the TransCom land regions to interpret regional carbon budgets, while flux estimations in their models are done at much higher spatial resolutions (e.g. Feng et al., 2009; Chevallier et al., 2010; Basu et al., 2013). Taking an advantage of being based on the CDIAC estimates, we adopted the updated uncertainty estimates reported by Andres et al. (2016) and obtained the regional uncertainty estimates. Those estimates are new and readily usable to the inversion studies especially when interpreting the regional estimates.

8. Product distribution, data policy and future update

The ODIAC2016 data product is available from a website hosted by the Center for Global Environmental Research (CGER), Japanese National Institute for Environmental Studies (NIES) (http://db.cger.nies.go.jp/dataset/ODIAC/, doi: 10.17595/20170411.001). The data product is distributed under Creative Commons Attribution 4.0 International (CC-BY 4.0, https://creativecommons.org/licenses/by/4.0/deed.en). The ODIAC2016 emission data are provided in two file formats: 1) global 1×1 km (30 arc second) monthly file in the GeoTIFF format (only includes emissions over land) and 2) 1×1 degree annual (12 month) file in the NetCDF format (includes international bunker emissions). A single, global 1×1 km monthly GeoTIFF file is about 3.7 GB (compressed to 120 MB). A 1×1 degree single NetCDF annual file is about 6MB.

We update the emission data on annual basis, following a release of an updated global fuel statistical data. Future versions of the emissions data are in principle based on updated version/edition of the underlying statistical data with the same name convention (ODIACYYYY, YYYY= the release year, the end year is YYYY minus 1). In October 2017, we started distributing the updated, year 2017 version of ODIAC data (ODIAC2017, 2000–2016). We primarily focus on years after 2000. Future versions of ODIAC data however might have a longer, extended time coverage.

9. Summary

This manuscript describes the year 2016 version of ODIAC emission data (ODIAC2016) and how the emission data product was developed within our upgraded emission modeling

framework. Based on the CDIAC emission data, ODIAC2016 can be viewed as an extended version of the CDIAC gridded data with improved emission spatial distributions representations. Utilizing the best available data (emission estimates and proxy), we achieved a comprehensive, global fossil fuel CO_2 gridded emission field that allows data users to impose their CO_2 simulations in a consistent way with many of the global carbon budget analysis. With updated fuel statistics, we should be able to continue producing an updated, future versions of ODIAC emission data product within the same model framework. The capability we developed in this study has become more significance now, given the CDIAC/ORNL's shutdown. Despise of expected difficulties (e.g. discontinued CDIAC estimates), the authors believe that ODIAC could play an important role in delivering emission data to the carbon cycle science community. Limitations and caveats discussed in this manuscript mirror and lead ODIAC's future prospects. The ODIAC emission data product is distributed from http://db.cger.nies.go.jp/dataset/ODIAC/ with a DOI. Currently the 2017 version of ODIAC emission data (ODIAC2017, 2000–2016) is also available.

Acknowledgments

TO is supported by NASA Carbon Cycle Science program (Grant # NNX14AM76G). RJA is now retired but this work was sponsored by U.S. Department of Energy, Office of Science, Biological and Environmental Research (BER) programs and performed at the Oak Ridge National Laboratory (ORNL) under U.S. Department of Energy contract DE-AC05–00OR22725. The authors would like to thank Chris Elvidge and Kim Baugh at NOAA/NGDC for providing the nightlight data. The authors also thank Yasuhiro Tsukada and Tomoko Shirai for hosting the ODIAC emission data on the data server at NIES.

Appendix A

Table A1.

A list of components in ODIAC2016 and data used in the development.

Component	Data/ product name	Description and data source	Reference
Global FFCO2	CDIAC global fossil-fuel CO_2 emissions	The year 2016 edition of the CDIAC global total estimates were used to constrain the ODIAC2016 totals. Data available at http://cdiac.ornl.gov/ ftp/ndp030/global.1751_2013.ems.	Boden et al. (2016)
National FFCO2	CDIAC fossil-fuel CO_2 emissions by Nation	The year 2016 editions of the CDIAC national emission estimates are used as a primary input data. Data available at http://cdiac.ornl.gov/ ftp/ndp030/nation.1751_2013.ems.	Boden et al. (2016)
Global fuel statistics	BP Statistical review of world energy	The year 2016 edition of the BP statistical data were used to project CDIAC national emissions over the recent years (2014–2015). Data are available at http://www.bp.com/en/global/corporate/energy-economics/statistical-review-of-world-energy.html.	BP (2017)
Monthly temporal variation	CDIAC Gridded Monthly Estimate	The year 2013 version of the CDIAC monthly gridded data were used to the model seasonality in ODIAC2016. Data are available at http://cdiac.ornl.gov/ ftp/fossil_fuel_CO2_emissions_gridded_monthly_v2013/	Andres et al. (2011)
Power plant data	CARMA	The CARMA power plant database with geolocation correction described in Oda and Maksyutov (2011). Data available from http://carma.org/.	Wheeler and Ummel et al. 2008

Component	Data/ product name	Description and data source	Reference
NTL (for non-point emissions)	Global Radiance Calibrated Nighttime Lights	Multiple year NTL data are used to distribute nonpoint emissions. Data are available at https://ngdc.noaa.gov/eog/dmsp/download_radcal.html.	Ziskin et al. (2010)
NTL (for gas flaring)	Global Gas Flaring Shapefiles	Global gas flaring NTL data are specifically used to distribute gas flaring emissions. Data are available at http://ngdc.noaa.gov/eog/interest/gas_flares_countries_shapefiles.html	Elvidge et al. (2009)
Int'l ship tracks	EDGAR v4.1	The international marine bunker emission field in EDGAR v4.1 was used. Data are available at http://edgar.jrc.ec.europa.eu/archived_datasets.php.	JRC (2017)
Int'l Aviation flight tracks	AERO2k	Data were used to distributed aviation emissions. More details can be find at http://www.cate.mmu.ac.uk/projects/aero2k/.	Eyers et al. (2005)
Weekly and diurnal cycle	TIMES	This was not a part of ODIAC2016, however it is useful to note that this scaling factors can be used to create weekly and diurnally varying emissions. Data are available at http://cdiac.ornl.gov/ftp/Nassar_Emissions_Scale_Factors/.	Nasar et al. (2013)

Appendix A2

Table A2.

A table for the global scaling factor for 2000–2013.

Year	Scaling factor
2000	0.999
2001	1.016
2002	1.008
2003	1.014
2004	1.012
2005	1.022
2006	1.022
2008	1.023
2009	1.024
2010	1.015
2011	1.017
2012	1.017
2013	1.025

Appendix A3

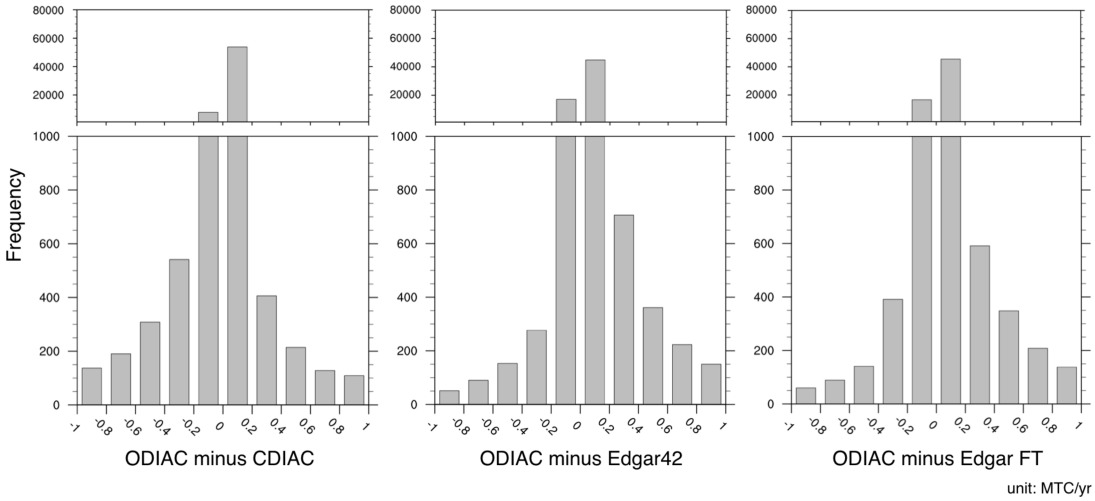

Fig. A3.

A histogram of the inter-emission data differences from ODIAC. Values are given in the unit of million tonnes carbon per year (MTC/yr).

References

Andres RJ, Marland G, Fung I, and Matthews E: A 1°× 1° distribution of carbon dioxide emissions from fossil fuel consumption and cement manufacture, 1950–1990, Global Biogeochem. Cycles, 10(3), 419–429, doi:10.1029/96GB01523, 1996.

Andres RJ, Gregg JS, Losey L, Marland G, and Boden TA: Monthly, global emissions of carbon dioxide from fossil fuel consumption. Tellus B, 63:309–327. doi:10.1111/j.1600-0889.2011.00530.x, 2011.

Andres RJ, Boden TA, Breon F-M, Ciais P, Davis S, Erickson D, Gregg JS, Jacobson A, Marland G, Miller J, Oda T, Olivier JGJ, Raupach MR, Rayner P, and Treanton K: A synthesis of carbon dioxide emissions from fossil-fuel combustion, Biogeosciences, 9, 1845–1871, doi:10.5194/bg-9-1845-2012, 2012.

Andres RJ, Boden TA, and Higdon D: A new evaluation of the uncertainty associated with CDIAC estimates of fossil fuel carbon dioxide emission. Tellus B Chem. Phys. Meterol. 66, 23616, 2014.

Andres RJ, Boden TA, and Higdon DM: Gridded uncertainty in fossil fuel carbon dioxide emission maps, a CDIAC example, Atmos. Chem. Phys. Discuss, doi:10.5194/acp-2016-258, in review, 2016.

Asefi-Najafabady S, Rayner PJ, Gurney KR, McRobert A, Song Y, Coltin K, Huang J, Elvidge C, and Baugh K: A multiyear, global gridded fossil fuel CO_2 emission data product: Evaluation and analysis of results, J. Geophys. Res. Atmos, 119, 10,213–10,231, doi:10.1002/2013JD021296, 2014.

Ballantyne AP, Alden CB, Miller JB, Tans PP and White JWC: Increase in observed net carbon dioxide uptake by land and oceans during the past 50 years, Nature, 488 (7409), 70–72, 2012. [PubMed: 22859203]

Baker DF, Doney SC and Schimel DS: Variational data assimilation for atmospheric CO_2. Tellus B, 58: 359–365. doi:10.1111/j.1600-0889.2006.00218.x, 2006.

Basu S, Guerlet S, Butz A, Houweling S, Hasekamp O, Aben I, Krummel P, Steele P, Langenfelds R, Torn M, Biraud S, Stephens B, Andrews A, and Worthy D: Global CO_2 fluxes estimated from GOSAT retrievals of total column CO_2, Atmos. Chem. Phys, 13, 8695–8717, doi:10.5194/acp-13-8695-2013, 2013.

Basu S, Miller JB, and Lehman S: Separation of biospheric and fossil fuel fluxes of CO_2 by atmospheric inversion of CO_2 and $^{14}CO_2$ measurements: Observation System Simulations, Atmos. Chem. Phys, 16, 5665–5683, doi:10.5194/acp-16-5665-2016, 2016.

Boden TA, Marland G, and Andres RJ: Global, Regional, and National Fossil-Fuel CO_2 Emissions. Carbon Dioxide Information Analysis Center, Oak Ridge National Laboratory, U.S. Department of Energy, Oak Ridge, Tenn., U.S.A. doi 10.3334/CDIAC/00001_V2015, 2015.

Boden TA, Marland G, and Andres RJ. 2016 Global, Regional, and National Fossil-Fuel CO_2 Emissions. Carbon Dioxide Information Analysis Center, Oak Ridge National Laboratory, U.S. Department of Energy, Oak Ridge, Tenn., U.S.A. doi 10.3334/CDIAC/00001_V2016

Boden TA, Marland G, and Andres RJ. 2017 Global, Regional, and National Fossil-Fuel CO_2 Emissions. Carbon Dioxide Information Analysis Center, Oak Ridge National Laboratory, U.S. Department of Energy, Oak Ridge, Tenn., U.S.A. doi 10.3334/CDIAC/00001_V2017

Bousquet P, Ciais P, Peylin P, Ramonet M and Monfray P: Inverse modeling of annual atmospheric CO_2 sources and sinks 1. Method and control inversion, J. Geophys. Res,104 (D21), 26161–26178, 1999.

Brioude J, Angevine WM, Ahmadov R, Kim S-W, Evan S, McKeen SA, Hsie EY, Frost GJ, Neuman JA, Pollack IB, Peischl J, Ryerson TB, Holloway J, Brown SS, Nowak JB, Roberts JM, Wofsy SC, Santoni GW, Oda T, and Trainer M: Top-down estimate of surface flux in the Los Angeles Basin using a mesoscale inverse modeling technique: assessing anthropogenic emissions of CO,NO_x and CO_2 and their impacts, Atmos. Chem. Phys, 13, 3661–3677, doi:10.5194/acp-13-3661-2013, 2013.

BP: Statistical Review of World Energy, available at http://www.bp.com/en/global/corporate/energy-economics/statistical-review-of-world-energy.html (last access: 6 June 2017), 2017.

Chevallier F, et al.: CO_2 surface fluxes at grid point scale estimated from a global 21 year reanalysis of atmospheric measurements, J. Geophys. Res, 115, D21307, doi: 10.1029/2010JD013887, 2010.

Doll CNH, Muller J-P, and Elvidge CD Nighttime imagery as a tool for global mapping of socioeconomic parameters and greenhouse gas emissions, Ambio, 29, 157–162, 2000.

Elvidge CD, Baugh KE, Dietz JB, Bland T, Sutton PC, and Kroehl HW: Radiance calibration of DMSP-OLS lowLight imaging data of human settlements - a new device for portraying the Earth's surface entire, Remote Sens. Environ, 68, 77–88, 1999.

Elvidge CD, Imhoff ML, Baugh KE, Hobson VR, Nelson I, Safran J, Dietz JB, and Tuttle BT: Night-time lights of the world: 1994–1995, J. Photogr. Remote Sens, 56, 81–99, 2001.

Elvidge CD, Ziskin D, Baugh KE, Tuttle BT, Ghosh T, Pack DW, Erwin EH, Zhizhin M: A Fifteen Year Record of Global Natural Gas Flaring Derived from Satellite Data. Energies, 2, 595–622, 2009.

Elvidge CD, Zhizhin M, Hsu F-C, and Baugh KE: VIIRS Nightfire: Satellite pyrometry at night, Remote Sensing, 5, 4423–4449, 2013a.

Elvidge CD, Baugh KE, Zhizhin M, and Hsu F-C: Why VIIRS data are superior to DMSP for mapping nighttime lights. Proceedings of the Asia-Pacific Advanced Network, 35, 62–69. doi: 10.7125/apan.35.7, 2013b.

EPA: Emissions and Generation Resource Integrated Database (eGRID), available at https://www.epa.gov/energy/emissions-generation-resource-integrated-database-egrid (last access: 6 June 2017), 2017

Eyers CJ, Norman P, Middel J, Plohr M, Michot S, Atkinson K, and Christou RA: AERO2k Global Aviation Emissions Inventories for 2002 and 2025, QinetiQ/04/001113, 2005.

Feng L, Palmer PI, Bosch H, and Dance S: Estimating surface CO_2 fluxes from space-borne CO_2 dry air mole fraction observations using an ensemble Kalman Filter, Atmos. Chem. Phys, 9, 2619–2633, 10.5194/acp-9-2619-2009, 2009.

Feng L, Palmer PI, Parker RJ, Deutscher NM, Feist DG, Kivi R, Morino I, and Sussmann R: Estimates of European uptake of CO_2 inferred from GOSAT X_{CO2} retrievals: sensitivity to measurement bias inside and outside Europe, Atmos. Chem. Phys, 16, 1289–1302, doi:10.5194/acp-16-1289-2016, 2016.

Feng S, Lauvaux T, Newman S, Rao P, Ahmadov R, Deng A, Diaz-Isaac LI, Duren RM, Fischer ML, Gerbig C, Gurney KR, Huang J, Jeong S, Li Z, Miller CE, O'Keeffe D, Patarasuk R, Sander SP, Song Y, Wong KW, and Yung YL: Los Angeles megacity: a high-resolution land-atmosphere modelling system for urban CO_2 emissions, Atmos. Chem. Phys, 16, 9019–9045, doi:10.5194/acp-16-9019-2016, 2016.

Feng L, Palmer PI, Bosch H, Parker RJ, Webb AJ, Correia CSC, Deutscher NM, Domingues LG, Feist DG, Gatti LV, Gloor E, Hase F, Kivi R, Liu Y, Miller JB, Morino I, Sussmann R, Strong K, Uchino O, Wang J, and Zahn A: Consistent regional fluxes of CH4 and CO_2 inferred from GOSAT proxy XCH4 : XCO_2 retrievals, 2010–2014, Atmos. Chem. Phys, 17, 4781–4797, doi:10.5194/acp-17-4781-2017, 2017.

Ganshin A, Oda T, Saito M, Maksyutov S, Valsala V, Andres RJ, Fisher RE, Lowry D, Lukyanov A, Matsueda H, Nisbet EG, Rigby M, Sawa Y, Toumi R, Tsuboi K, Varlagin A, and Zhuravlev R: A global coupled Eulerian-Lagrangian model and 1 × 1 km CO_2 surface flux dataset for high-resolution atmospheric CO_2 transport simulations, Geosci. Model Dev, 5, 231–243, 10.5194/gmd-5-231-2012, 2012.

Ghosh T, Elvidge CD, Sutton PC, Baugh KE, Ziskin D, and Tuttle BT: Creating a Global Grid of Distributed Fossil Fuel CO_2 Emissions from Nighttime Satellite Imagery. Energies, 3, 1895–1913, 2010.

Gurney KR, Law RM, Denning AS, Rayner PJ, Baker D, Bousquet P, Bruhwiler L, Chen YH, Ciais P, Fan S, Fung IY, Gloor M, Heimann M, Higuchi K, John J, Maki T, Maksyutov S, Masarie K, Peylin P, Prather M, Pak BC, Randerson J, Sarmiento J, Taguchi S, Takahashi T, and Yuen CW: Towards robust regional estimates of CO_2 sources and sinks using atmospheric transport models, Nature, 415, 626–630, 2002. [PubMed: 11832942]

Gumey KR, Chen Y-H, Maki T, Kawa SR, Andrews A, and Zhu Z: Sensitivity of atmospheric CO_2 inversions to seasonal and interannual variations in fossil fuel emissions, J. Geophys. Res, 110, D10308, doi: 10.1029/2004JD005373, 2005.

Gurney KR, Mendoza D, Zhou Y, Fischer M, de la Rue du Can, S., Geethakumar, S., Miller, C.: The Vulcan Project: High resolution fossil fuel combustion CO_2 emissions fluxes for the United States, Environ. Sci. Technol, 43, doi:10.1021/es900806c, 2009.

Gurney K, Razlivanov I, Song Y, Zhou Y. et al. 2012 Quantification of fossil fuel CO_2 emission on the building/street scale for a large US city. Environ. Sci. & Technol 46: 12194–12202. [PubMed: 22891924]

Hakkarainen J, Ialongo I, and Tamminen J (2016), Direct space-based observations of anthropogenic CO2 emission areas from OCO-2, Geophys. Res. Lett, 43, 11,400–11,406, doi: 10.1002/2016GL070885.

Hogue S, Marland E, Andres RJ, Marland G, and Woodard D: Uncertainty in gridded CO_2 emissions estimates, Earth's Future, 4, 225–239, doi: 10.1002/2015EF000343, 2016.

Hutchins MG, Colby JD, Marland G and Marland E: A comparison of five high-resolution spatially-explicit, fossil-fuel, carbon dioxide emission inventories for the United States, Mitig Adapt Strateg Glob Change,. doi:10.1007/s11027-016-9709-9, 2016

Janardanan R, Maksyutov S, Oda T, Saito M, Kaiser JW, Ganshin A, Stohl A, Matsunaga T, Yoshida Y, and Yokota T: Comparing GOSAT observations of localized CO_2 enhancements by large emitters with inventory-based estimates, Geophys. Res. Lett, 43, 3486–3493, doi:10.1002/2016GL067843, 2016.

Janssens-Maenhout G, Dentener F, Van Aardenne J, Monni S, Pagliari V, Orlandini L, Klimont Z, Kurokawa J, Akimoto H, Ohara T, Wankmueller R, Battye B, Grano D; Zuber A, Keating T. EDGAR-HTAP: a Harmonized Gridded Air Pollution Emission Dataset Based on National Inventories. Ispra (Italy): European Commission Publications Office; 2012 JRC68434, EUR report No EUR 25 299 – 2012, ISBN 978–92-79–23122-0, ISSN 1831–9424

JRC: EDGAR - Emissions Database for Global Atmospheric Research, available at http://edgar.jrc.ec.europa.eu/ (last access: June 2017), 2017.

Kurokawa J, Ohara T, Morikawa T, Hanayama S, Janssens-Maenhout G, Fukui T, Kawashima K, and Akimoto H: Emissions of air pollutants and greenhouse gases over Asian regions during 2000–2008: Regional Emission inventory in ASia (REAS) version 2, Atmos. Chem. Phys, 13, 11019–11058, doi:10.5194/acp-13-11019-2013, 2013.

Lauvaux T, et al.: High-resolution atmospheric inversion of urban CO_2 emissions during the dormant season of the Indianapolis Flux Experiment (INFLUX), J. Geophys. Res. Atmos, 121, doi: 10.1002/2015JD024473, 2016.

Le Quéré C, Andrew RM, Canadell JG, Sitch S, Korsbakken JI, Peters GP, Manning AC, Boden TA, Tans PP, Houghton RA, Keeling RF, Alin S, Andrews OD, Anthoni P, Barbero L, Bopp L,

Chevallier F, Chini LP, Ciais P, Currie K, Delire C, Doney SC, Friedlingstein P, Gkritzalis T, Harris I, Hauck J, Haverd V, Hoppema M, Klein Goldewijk K, Jain AK, Kato E, Kortzinger A, Landschutzer P, Lefevre N, Lenton A, Lienert S, Lombardozzi D, Melton JR, Metzl N, Millero F, Monteiro PMS, Munro DR, Nabel JEMS, Nakaoka SI, O'Brien K, Olsen A, Omar AM, Ono T, Pierrot D, Poulter B, Rodenbeck C, Salisbury J, Schuster U, Schwinger J, Seferian R, Skjelvan I, Stocker BD, Sutton AJ, Takahashi T, Tian H, Tilbrook B, van der Laan-Luijkx IT, van der Werf GR, Viovy N, Walker AP, Wiltshire AJ, and Zaehle S: Global Carbon Budget 2016, Earth Syst. Sci. Data, 8, 605–649, doi:10.5194/essd-8-605-2016, 2016.

Maksyutov S, Takagi H, Valsala VK, Saito M, Oda T, Saeki T, Belikov DA, Saito R, Ito A, Yoshida Y, Morino I, Uchino O, Andres RJ, and Yokota T: Regional CO_2 flux estimates for 2009–2010 based on GOSAT and ground-based CO_2 observations, Atmos. Chem. Phys, 13, 9351–9373, doi: 10.5194/acp-13-9351-2013, 2013.

Marland G, and Rotty RM: Carbon dioxide emissions from fossil fuels: a procedure for estimation and results for 1950–1982. Tellus B, 36B: 232–261. doi: 10.1111/j.1600-0889.1984.tb00245.x, 1984.

Myhre G, Alterskjær K, and Lowe D: A fast method for updating global fossil fuel carbon dioxide emissions, Environ. Res. Lett, 4, 034012, doi:10.1088/1748-9326/4/3/034012, 2009.

Nassar R, Jones DBA, Suntharalingam P, Chen JM, Andres RJ, Wecht KJ, Yantosca RM, Kulawik SS, Bowman KW, Worden JR, Machida T, and Matsueda H: Modeling global atmospheric CO_2 with improved emission inventories and CO_2production from the oxidation of other carbon species, Geosci. Model Dev, 3, 689716, doi:10.5194/gmd-3-689-2010, 2010.

Nassar R, Napier-Linton L, Gurney KR, Andres RJ, Oda T, Vogel FR, and Deng F: Improving the temporal and spatial distribution of $_{CO2}$ emissions from global fossil fuel emission data sets, J. Geophys. Res. Atmos, 118, 917–933, doi:10.1029/2012JD018196, 2013.

Oda T, Maksyutov S, and Elvidge CD: Disaggregation of national fossil fuel CO_2 emissions using a global power plant database and DMSP nightlight data, Proc. of the Asia Pacific Advanced Network, 30, 220–229, 2010.

Oda T and Maksyutov S: A very high-resolution (1 km×1 km) global fossil fuel CO_2 emission inventory derived using a point source database and satellite observations of nighttime lights, Atmos. Chem. Phys, 11, 543–556, doi:10.5194/acp-11-543-2011, 2011.

Oda T, Ganshin A, Saito M, Andres RJ, Zhuravlev R, Sawa Y, Fisher RE, Rigby M, Lowry D, Tsuboi K, Matsueda H, Nisbet EG, Toumi R, Lukyanov A, and Maksyutov S: The use of a high-resolution emission dataset in a Global Eulerian-Lagrangian coupled model, "Lagrangian Modeling of the Atmosphere", AGU Geophysical monograph series, 2012.

Oda T and Maksyutov S: Open-source Data Inventory for Anthropogenic CO2 (ODIAC) emission dataset, National Institute for Environmental Studies, Tsukuba, Japan. doi: 10.17595/20170411.001, URL: http://db.cger.nies.go.jp/dataset/ODIAC/

Oda T, Ott L, Topylko P, Halushchak M, Bun R, Lesiv M, Danylo O and Horabik-Pyzel J: Uncertainty associated with fossil fuel carbon dioxide (CO_2) gridded emission datasets. In: Proceedings, 4th International Workshop on Uncertainty in Atmospheric Emissions, 7–9 October 2015, Krakow, Poland Systems Research Institute, Polish Academy of Sciences, Warsaw, Poland, pp. 124–129. ISBN 83–894-7557-X

Oda T, et al.: On the impact of granularity of space-based urban CO2 emissions in urban atmospheric inversions: A case study for Indianapolis, IN. Elem Sci Anth, 5: 28, DOI: 10.1525/elementa.146, 2017

Olsen SC, Wuebbles DJ, and Owen B: Comparison of global 3-D aviation emissions datasets, Atmos. Chem. Phys, 13, 429–441, doi:10.5194/acp-13-429-2013, 2013.

Peters W, Jacobson AR, Sweeney C, Andrews AE, Conway TJ, Masrie K, Miller JB, Bruhwiler LM, Petron G, Hirsch AI, Worthy DE, van der Werf GR, Randerson JT, Wennberg PO, Krol MC and Tans PP: An atmospheric perspective on North American carbon dioxide exchange: CarbonTracker, PNAS, 11 27, 2007, vol. 104, no. 48, 18925–18930, 2007. [PubMed: 18045791]

Peylin P, Law RM, Gurney KR, Chevallier F, Jacobson AR, Maki T, Niwa Y, Patra PK, Peters W, Rayner PJ, Rodenbeck C, van der Laan-Luijkx IT, and Zhang X: Global atmospheric carbon budget: results from an ensemble of atmospheric CO_2 inversions, Biogeosciences, 10, 6699–6720, doi:10.5194/bg-10-6699-2013, 2013.

Raupach MR, Rayner PJ, and Paget M: Regional variations in spatial structure of nightlights, population density and fossil-fuel CO_2 emissions, Energy Policy, 38, 4756–4764, doi:10.1016/j.enpol.2009.08.021, 2010.

Rayner PJ, Raupach MR, Paget M, Peylin P, and Koffi E: A new global gridded data set of CO_2 emissions from fossil fuel combustion: Methodology and evaluation, J. Geophys. Res, 115, D19306, doi:10.1029/2009JD013439, 2010.

Roman MO, and Stokes EC: Holidays in Lights: Tracking cultural patterns in demand for energy services, Earth's Future, doi:10.1002/2014EF000285, 2015.

Saeki T, Maksyutov S, Sasakawa M, Machida T, Arshinov M, Tans P, Conway TJ, Saito M, Valsala V, Oda T, Andres RJ, and Belikov D: Carbon flux estimation for Siberia by inverse modeling constrained by aircraft and tower CO2 measurements, J. Geophys. Res. Atmos, 118, 1100–1122, doi:10.1002/jgrd.50127, 2013.

Schneising O, Heymann J, Buchwitz M, Reuter M, Bovensmann H, and Burrows JP: Anthropogenic carbon dioxide source areas observed from space: assessment of regional enhancements and trends, Atmos. Chem. Phys, 13, 2445–2454, doi:10.5194/acp-13-2445-2013, 2013

Shrai T, Ishizawa M, Zhuravlev R, Ganshin A, Belikov D, Saito M, Oda T, Valsala V, Gomez-Pelaez AJ, Langenfelds R and Maksyutov S: A decadal inversion of CO2 using the Global Eulerian-Lagrangian Coupled Atmospheric model (GELCA): Sensitivity to the ground-based observation network, Tellus B: Chemical and Physical Meteorology, 69:1,129–1,158, DOI: 10.1080/16000889.2017.1291158, 2017

Takagi H, Saeki T, Oda T, Saito M, Valsala V, Belikov D, Saito R, Yoshida Y, Morino I, Uchino O, Andres RJ, Yokota T, and Maksyutov S: On the benefit of GOSAT observations to the estimation of regional CO_2 fluxes, SOLA, 7, 161–164, 2009.

Tans PP, Fung IY and Enting IG: Observational constraints on the global atmospheric CO_2 budget, Science, 247, 1431–1438, 1990. [PubMed: 17791210]

Thompson RL, Patra PK, Chevallier F, Maksyutov S, Law RM, Ziehn T, Laan-Luijkx IT, Peters W, Ganshin A, Zhuravlev R, Maki T, Nakamura T, Shirai T, Ishizawa M, Saeki T, Machida T, Poulter B, Canadell JG, and Ciais P: Top-down assessment of the Asian carbon budget since the mid 1990s, Nature Comm, 7, 2016.

Vogel F, Tiruchittampalam B, Theloke J, Kretschmer R, Gerbig C, Hammer S, and Levin I, : Can we evaluate a fine-grained emission model using high-resolution atmospheric transport modelling and regional fossil fuel CO_2 observations?. Tellus B, 65. doi:10.3402/tellusb.v65i0.18681, 2013.

Wheeler D and Ummel K: Calculating CARMA: Global Estimation of CO_2 Emissions From the Power Sector, https://www.cgdev.org/publication/calculating-carma-global-estimation-co2-emissions-power-sector-working-paper-145, 2008.

Woodard D, Branham M, Buckingham G, Hogue S, Hutchins M, Gosky R, Marland G, and Marland E: A spatial uncertainty metric for anthropogenic CO_2 emissions, Greenhouse GasMeas. Manage., doi:10.1080/20430779.2014.1000793, 2015

Yokota T, Yoshida Y, Eguchi N, Ota Y, Tanaka T, Watanabe H, and Maksyutov S: Global concentrations of CO_2 and CH_4 retrieved from GOSAT: First preliminary results, SOLA, 5, 160–163, doi:10.2151/sola.2009-041, 2009.

Zhang X, Gurney KR, Rayner P, Liu Y, and Asefi-Najafabady S: Sensitivity of simulated CO_2 concentration to regridding of global fossil fuel CO_2 emissions, Geosci. Model Dev, 7, 2867–2874, doi:10.5194/gmd-7-2867-2014, 2014

Ziskin D, Baugh K, Hsu F-C, Ghosh T, Elvidege C: Methods Used For the 2006 Radiance Lights, Proc. of the 30th Asia-Pacific Advanced Network Meeting, 131–14, 2010.

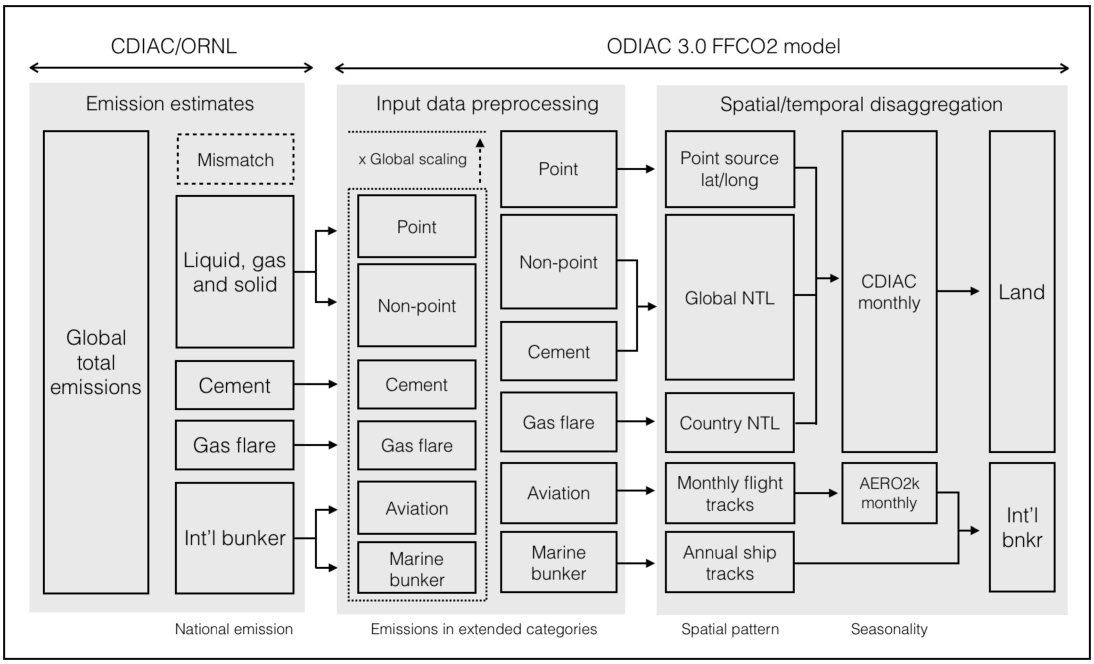

Figure 1.

A schematic figure of the ODIAC emission modeling framework (defined as "ODIAC 3.0 FFCO2 model"). Starting with CDIAC national emission estimates made by fuel type (emission estimates), the CDIAC national emission estimates are first divided into extended ODIAC emission categories (input data processing, see Section 3). ODIAC 3.0 FFCO2 model then distributes the emissions in space and time, using point source geolocation information and spatial data depending on emission category such as nighttime light (NTL), and aircraft and ship fleet tracks (spatial disaggregation, see Section 4). The emission seasonality for emissions over land and international aviation were adopted from existing emission inventories (temporal disaggregation, see Section 5).

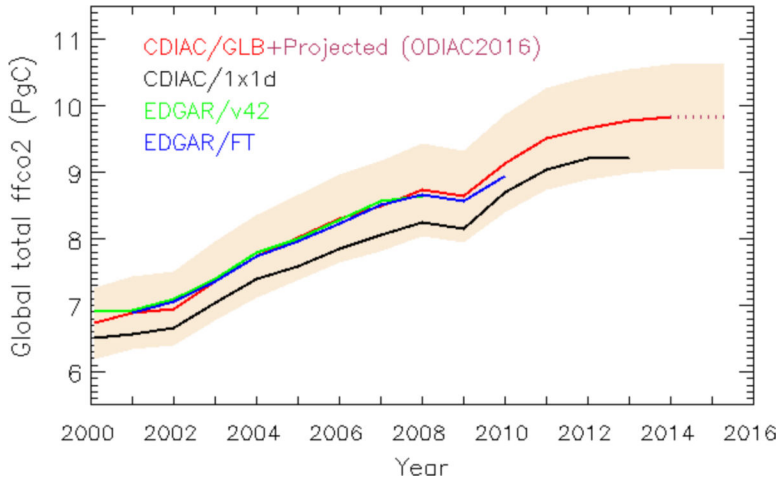

Figure 2.

Global emission time series from four gridded emission data: CDIAC (red, 2000–2013) plus projected emissions (dashed maroon, 2014–2015) (values taken from ODIAC2016), CDIAC 1×1 degree (black, 2000–2013), EDGAR v4.2 (green, 2000–2008) and EDGAR v4.2 Fast Track (blue, 2000–2010). The values here are given in the unit of peta gram (= giga tonnes) carbon per year. The shaded area indicated in tan is a two-sigma uncertainty range (8%) estimated for CDIAC global total emission estimates by Andres et al. (2014).

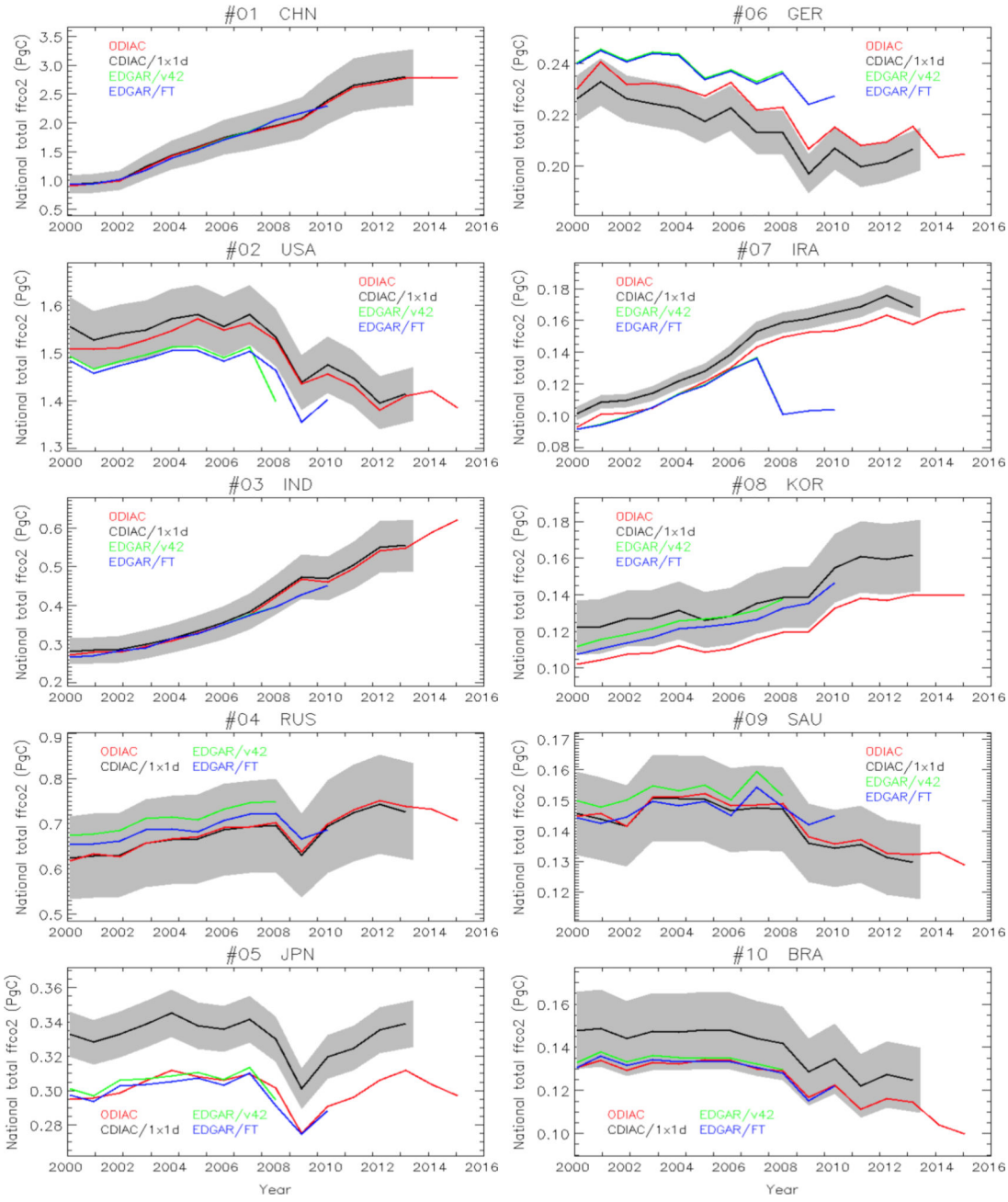

Figure 3.

National emission time series for top 10 emitting countries (China, U.S., India, Russian Federation, Japan, Germany, Islamic Republic of Iran, Republic of Korea (South Korea), Saudi Arabia and Brazil). The values are given in the unit of peta gram (=giga tonnes) carbon per year. The values are calculated using gridded emission data, not tabular emission data. The national total values in the plots might be thus different from values indicated in the tabular form due to the emission disaggregation. The shaded area in grey indicates a two-sigma uncertainty range estimated by Andres et al. (2014) (see Table 2).

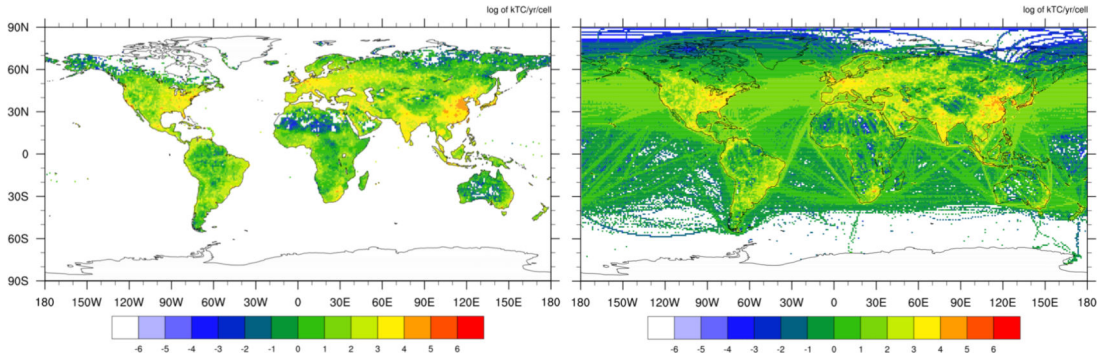

Figure 4.

Year 2013 global fossil fuel CO_2 emissions distributions from CDIAC (left, 8.36 PgC) and ODIAC (right, 9.78 PgC). The ODIAC emission field was aggregated to a common 1×1 degree resolution. The value is given in the unit of log of thousand tonnes C/cell.

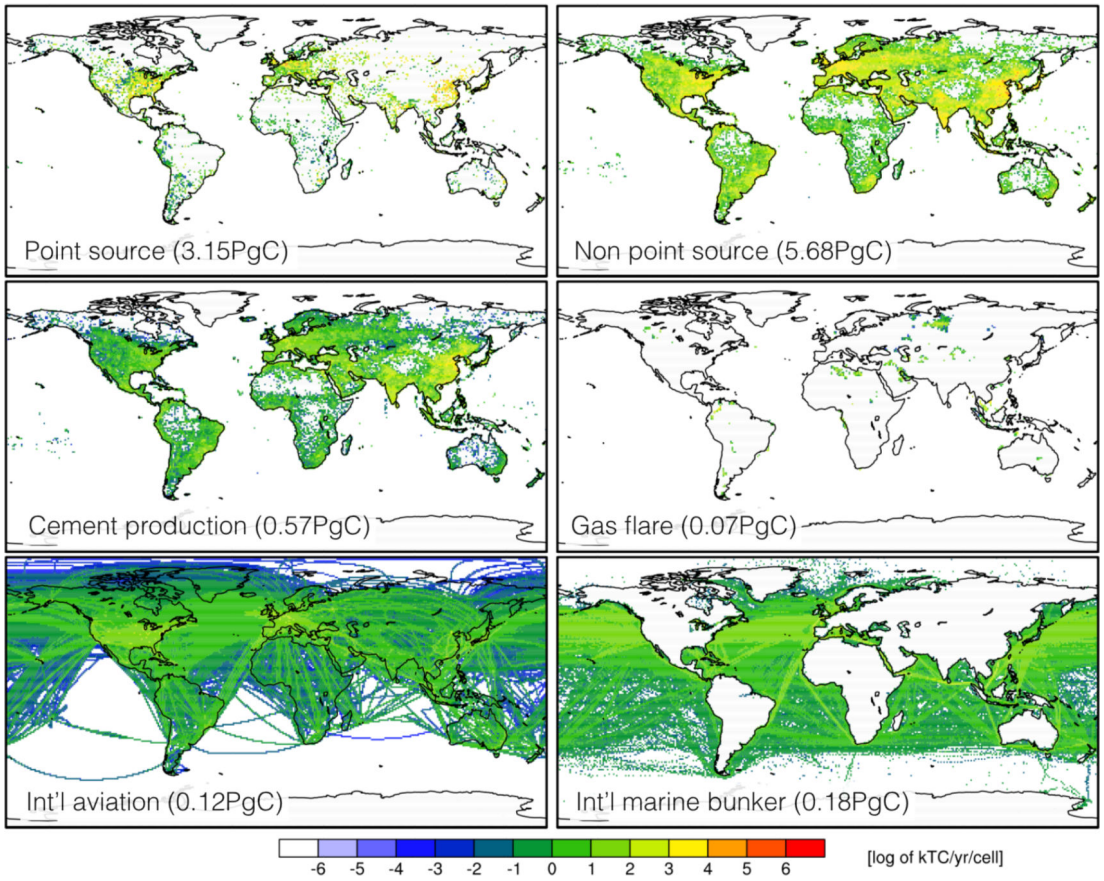

Figure 5.

Year 2013 global distributions of ODIAC fossil fuel emissions by emission type.The panels show emissions from (from top to the right, then down) point source, non-point source, cement production, gas flaring, international aviation and international shipping. The values in the figures are given in the unit of log of thousand tonnes carbon/year/cell (1×1 degree). The numbers in the brackets are the total for the category emissions in the unit of PgC (total year 2013 emission in ODIAC2016 was 9.78 PgC).

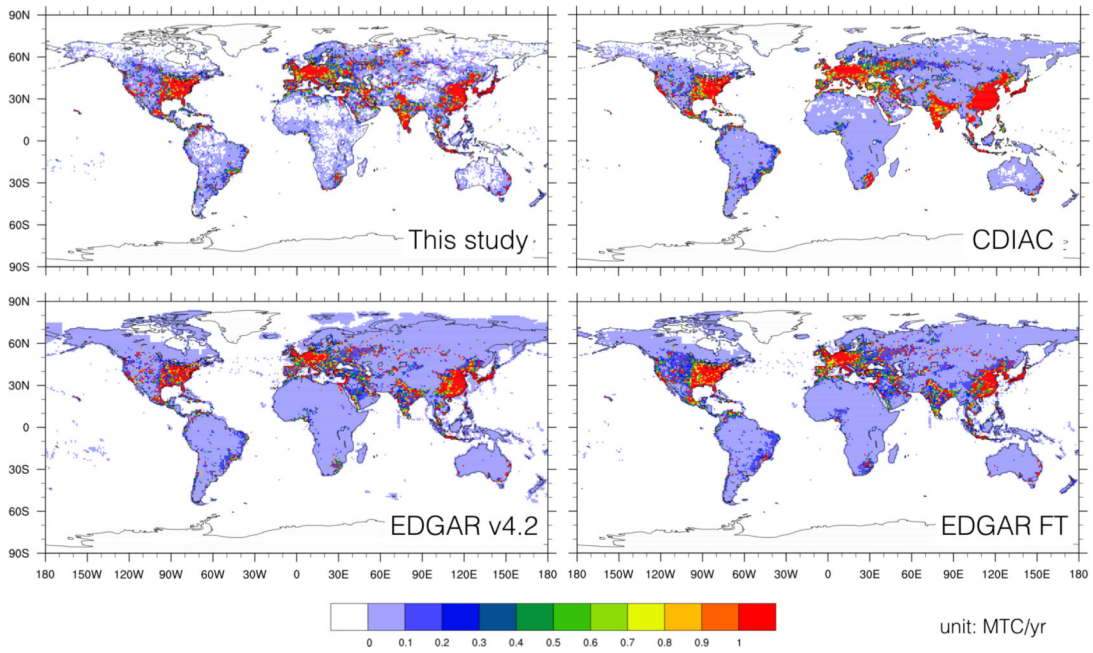

Figure 6.

Land emissions from ODIAC (upper left), CDIAC (upper right), two versions of EDGAR emission data (v4.2 lower left and v4.2 Fast Track lower right). The units are million tonnes carbon/year/cell (1×1 degree). In addition to excluding emissions from international aviation and marine bunker, some of the sector emissions were subtracted from EDGAR short cycle total emissions to account for the differences in emission calculation methods between CDIAC and EDGAR, as also done earlier. The emission fields for the year 2008 were used.

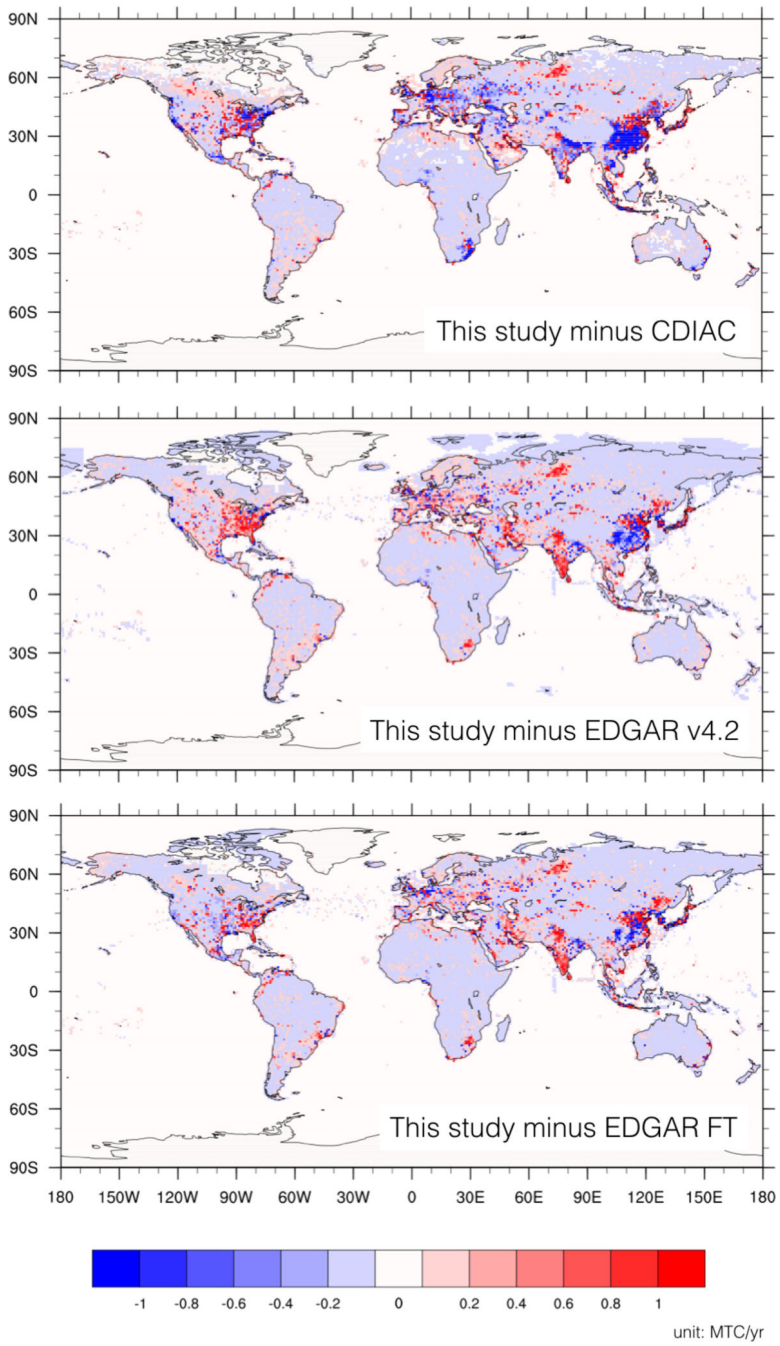

Figure 7.

ODIAC-other emission data differences. CDIAC (upper right), two versions of EDGAR (v4.2 lower left and v4.2 Fast Track lower right). The units are million tonnes carbon/year/cell (1×1 degree). Note that the differences are defined as ODIAC (this study) minus others. The histograms of the differences are also presented in Appendix A3.

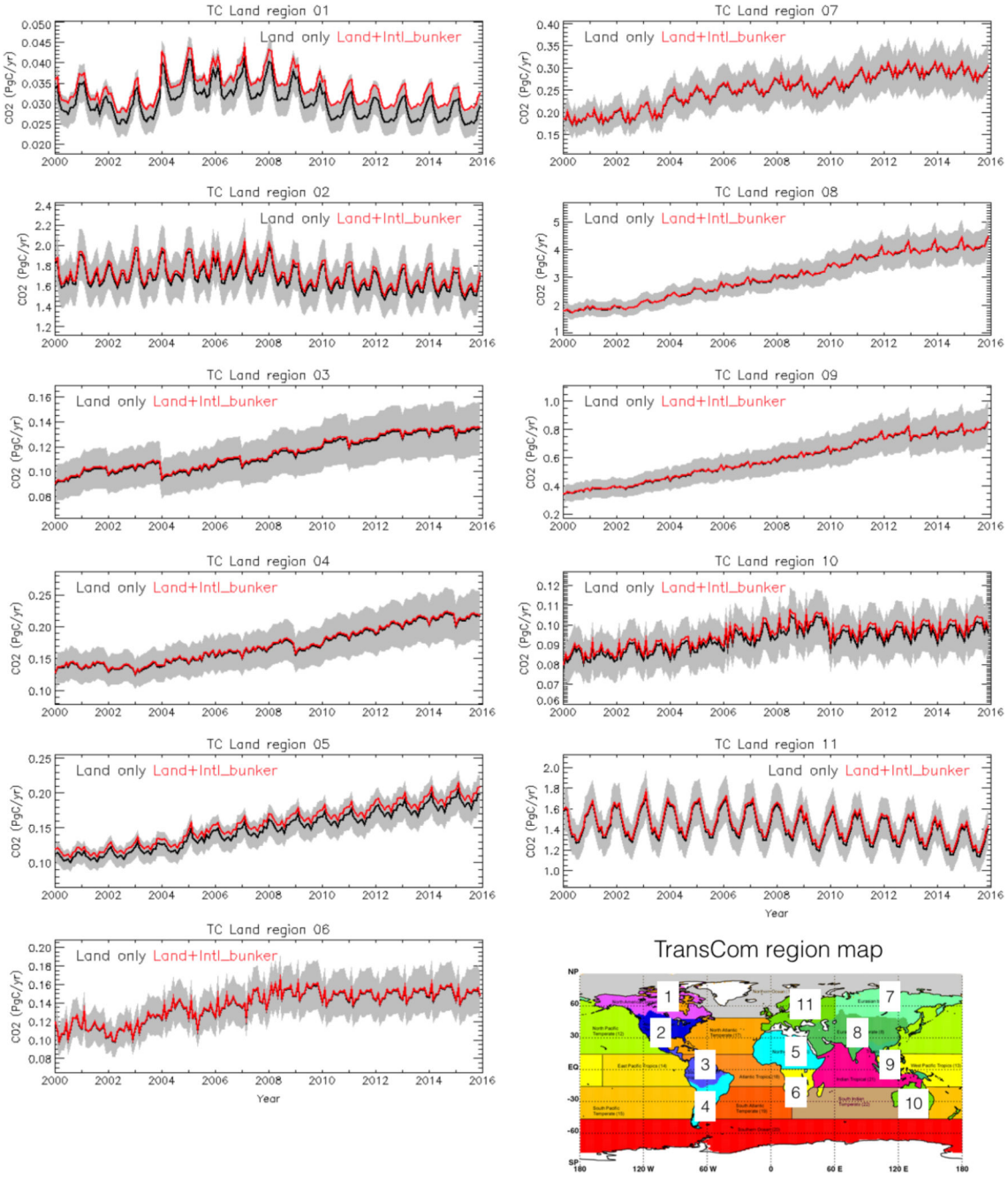

Figure 8.

Emission time series over inversion analysis land regions defined by the Transport model intercomparison (TransCom) project (Gurney et al., 2002). The TransCom region map (bottom right) is available fromhttp://transcom.project.asu.edu/transcom03 protocol basisMap.php (last access: 8 November, 2016). Black lines indicate the ODIAC 1×1 degree monthly emissions. The monthly emissions are calculated using the 1×1 degree ODIAC emission data. The uncertainty range was calculated by mass weighted uncertainty estimates of countries that fall into the regions (see Table 3). The uncertainty ranges shown in Fig. 8

are annual uncertainty plus the monthly profile uncertainty (12.8%, reported by Andres et al., 2011). Note scales in the vertical axis are different.

Table 1.

Global total emission estimates for year 2000, 2005 and 2010 from four gridded emission data (ODIAC2016, CDIAC, EDGAR v4.2 and EDGAR FastTrack). Values for two versions of EDGAR emission data were calculated by subtracting emissions from agriculture (IPCC code: 4C and 4D), land use change and forestry (5A, C, D, F and 4E) and waste (6C) from the total EDGAR CO_2 emissions (total short cycle C).

Year	ODIAC2016	CDIAC national	EDGAR v4.2	EDGAR FT
2000	6727	6506 (−3.3%)	6907 (+2.7%)	N/A
2005	8025	7592 (−5.4%)	8005 (−0.2%)	7959 (−0.8%)
2010	9137	8694 (−4.8%)	N/A	8950 (−2.0%)

Table 2.

Annual uncertainty estimates associated with CDIAC national emission estimates. The uncertainty estimates were made following the method described by Andres et al. (2014). The national total emissions for the year 2013 were taken from Boden et al. (2016).

Ranking #	Country	2013 emissions in kTC (% of the global total)	Uncertainty (%)
1	China	2,795,054 (28.6%)	17.5
2	U.S.	1,414,281 (14.5%)	4.0
3	India	554,882 (5.7%)	12.1
4	Russia Federation	487,885 (5.0%)	14.8
5	Japan	339,074 (3.5%)	4.0
6	Germany	206,521 (2.1%)	4.0
7	Islamic Republic of Iran	168,251 (1.7%)	9.4
8	Republic of Korea	161,576 (1.7%)	12.1
9	Saudi Arabia	147,649 (1.5%)	9.4
10	Brazil	137,354 (1.4%)	12.1

Table 3.

Annual total emission over the TransCom land regions and the associated uncertainty estimates. The total emissions were calculated using the ODIAD2016 gridded emission data. The numbers in the bracket are values including international bunker emissions. The uncertainty estimates were mass weighted values of uncertainty estimates of countries that fall in the regions. Country uncertainty estimates were estimated using the method described Andres et al. (2014). The values were reported as the 2-sigma uncertainty.

Region #	Region name	Uncertainty (%)
1	North American Boreal	3.7
2	North American Temperate	3.7
3	South American Tropical	9.6
4	South American Temperate	12.8
5	Northern Africa	5.1
6	Southern Africa	10.6
7	Eurasian Boreal	12.4
8	Eurasian Temperate	7.8
9	Tropical Asia	11.8
10	Australia	4.0
11	Europe	3.8